The Electronic Structure of Alkali Aurides. A Four-Component Dirac−Kohn−Sham Study

Leonardo Belpassi,* Francesco Tarantelli, and Antonio Sgamellotti

Dipartimento di Chimica e I.S.T.M.-C.N.R., Università di Perugia, 06123, Italy

Harry M. Quiney

ARC Centre of Excellence for Coherent X-ray Science, School of Physics, The University of Melbourne, Victoria, 3010, Australia

Received: September 1, 2005; In Final Form: February 2, 2006

Spectroscopic constants, including dissociation energies, harmonic and anharmonic vibrational frequencies, and dipole moments, are calculated for the complete alkali auride series (LiAu, NaAu, KAu, RbAu, CsAu). The four-component formulation of relativistic density functional theory has been employed in this study, using the *G*-spinor basis sets implemented recently in the program BERTHA. The performance of four standard nonrelativistic density functionals employed is investigated by comparing the results with the best available theoretical and experimental data. The present work provides the first theoretical predictions on the molecular properties of RbAu. The intermetallic bond that occurs in the alkali auride series is highly polar and is characterized by a large charge transfer from the alkali metals to gold. The extent of this electron transfer has been investigated using several different charge analysis methods, enabling us to reach some general conclusions on their relative performance. We further report a detailed analysis of the topological properties of relativistic electron density in the bonding region, discussing the features of this approach which characterize the nature of the chemical bond. We have also computed the fully relativistic density for the alkali halides MBr and MI (M = Li, Na, K, Rb, and Cs). The comparative study shows that, on the basis of several topological properties and the variation in bond lengths, the gold atom behaves similarly to a halogen intermediate between Br and I.

I. Introduction

In recent years, molecules and solids containing intermetallic bonds of the late transition metals have been studied with growing interest in solid, liquid, cluster, and gas-phase chemistry. This attention is motivated by the technological applications that mixed-metal compounds have in fields such as microelectronics, catalysis,[1] and nanostructured materials.[2] A particularly interesting case of intermetallic compounds is those containing gold.[3−8] Gold shows high polarizability and electronegativity, and it can take part in chemical bonds of different kinds, giving origin to a particularly rich chemistry in both molecules and clusters and on solid surfaces.[9−12] The geometry and energetics of these compounds are strongly influenced by relativity, electron correlation, and the so-called aurophilic effect.[13] These compounds exhibit peculiar features that result from the interplay between electronic and geometric effects in determining the size−stability balance. The study of the intermetallic bond in isolated molecules is very useful in providing insight into the nature and features of the bonding and has the advantage that it can be easily modeled and tracked both experimentally and theoretically.[14]

Due to the especially high difference in electronegativity between gold and alkali metals, the alkali aurides are found to be particularly stable, and it has recently been shown that the intermetallic bond between gold and the rare earths is particularly stable.[5] The nature of the intermetallic bond between alkali metals and gold has been the subject of various experimental and theoretical investigations, since the solid compounds CsAu and RbAu were discovered by Sommer.[15,16] Single-crystal data for RbAu and CsAu have been available since 1993.[17] Both CsAu and RbAu alloys crystallize with a cubic CsCl structure. The gold−lithium phase diagram is more complex, and in the range near the composition 1:1, there is a phase with CsCl structure as well as a phase with tetragonal structure.[18] The potassium and sodium alloys with gold in 1:1 stoichiometry do not exist.[18] The electrical properties change dramatically along the alkali metal series, and a metal−insulator transition occurs upon going from KAu to RbAu. Both CsAu and RbAu are ionic semiconductors. The stoichiometric compounds of Au with Li, Na, and K, on the other hand, are metals.[19] Theoretical band structure studies[19,20] indicate that it is not possible to reproduce these properties without including relativistic effects. In particular, Watson[21] showed that the semiconducting gap in solid CsAu and RbAu originates from a combination of the Au−Au separation and the ionic character of the compounds, and that the conductive properties of the Au−alkali metal compounds cannot be understood without including both relativistic effects and the changes in Au−Au separation. CsAu and RbAu in the liquid phase form an ionic melt[22,23] with a very low conductivity, reflecting the low mobility of the Cs^+, Rb^+, and Au^- ions. Molecular dynamics simulations have been published for liquid CsAu.[24,25] LiAu and NaAu, on the other hand, show metallic character in both the solid and liquid states. CsAu−ammonia (1:1), $CsAu{\cdot}NH_3$, has also recently been studied.[26] Diatomic molecular species of alkali aurides exist in the gas phase, and a number of experimental studies confirm their stabilities. The Knudsen cell method combined with mass spectroscopy analysis of the vapor composition has been the most successful experi-

* Email: belp@thch.unipg.it.

10.1021/jp054938w CCC: $33.50
Published on Web 03/09/2006

mental approach to the characterization of these compounds. Recently, two-photon ionization experiments have also been carried out.[27] The analysis, by the third-law method, of the high-temperature gaseous equilibria that takes place between gold and the alkali metals in the Knudsen cell mass spectroscopy experiment allowed the determination of the dissociation energies of most of the alkali aurides. The technique has been applied recently by Balducci et al.[5] to the study of the intermetallic bond in the diatomic molecules formed by gold and some rare earths. More than 30 years ago, the LiAu and NaAu molecules were observed, respectively, by Neubert[28] and Piacente,[29] while CsAu and RbAu were studied by Busse and Weil[30−32] in the early 1980s. There are no Knudsen cell mass spectroscopy experiments on KAu in the literature, but two-photon ionization experiments have recently led to the first direct observation of this molecule,[27] as well as of NaAu. The species have been produced by laser evaporation of a "salted" gold rod in a pulsed nozzle cluster source, and from the analysis of the spectra, it has been possible to determine the vibrational constants of the exited states and, in the case of KAu, also the ground-state fundamental frequency. Furthermore, the ground-state dissociation energies for NaAu and KAu have been determined. In the case of NaAu, the value obtained of 2.64 (±0.2) eV[27] differs significantly from that derived by the Knudsen cell mass spectroscopy experiments of 2.20 (±0.13) eV.[29]

The alkali aurides present special challenges to theoretical studies because of the large number of electrons and the importance of relativistic effects.[33] A comprehensive review of the current state-of-the-art of theoretical calculations for gold compounds is available in ref 14. Among the alkali aurides, CsAu has been the target of widest interest and has become a de facto test molecule to validate and calibrate different theoretical electronic structure models. Many theoretical investigations of this system have included relativistic corrections, either in a scalar model or in the full four-component formalism of the Dirac equation.[34−38] Fossgaard et al.,[38] for example, performed an extensive study of the effects of relativity, electron correlation, and the lanthanide contraction on the ground-state spectroscopic constants of CsAu. The calculations were performed using both wave function-based methods and density functional methods, both in the four-component formulation and in the corresponding nonrelativistic limit. The authors showed that, when electron correlation and relativity are combined, excellent agreement with the experimentally derived value for the dissociation energy is achieved. The molecule was found to be strongly polar, with a very high dipole moment. The analysis of the relativistic four-component Hartree−Fock wave function revealed a large charge transfer from the cesium atom to gold.

Theoretical studies are more scarce for the other alkali aurides. Schwerdtfeger et al.[33] examined the LiAu and NaAu molecules in a study of the relativistic and correlation effects in various diatomic gold compounds. Recently, Tong and Gheung[39] studed the diatomic molecules formed by the alkali metals (Li, Na, K) and the coinage metals (Cu, Ag, Au). They calculated different molecular properties using correlated methods based both on density functional and coupled-cluster theories. Relativistic effective core potentials were employed in the calculations. To our knowledge, no theoretical study has been reported of RbAu.

Recently, we completed the implementation of the generalized gradient approximation (GGA) within a four-component formulation of relativistic density functional theory[40] that is incorporated in the parallel version[41] of the program BERTHA.[42] In this recent work, we investigated the sensitivity of our results to the details of the numerical scheme used to evaluate the matrix elements, and we carried out a comparative study on CsAu using several standard nonrelativistic exchange-correlation functionals. It was shown that the performance of our implementation of the four-component Dirac−Kohn−Sham (DKS) approach is comparable to that of nonrelativistic density functional methods, and its reliable estimates of molecular parameters makes it an attractive alternative, also within the relativistic framework, to more expensive many-body techniques.

In the present work, we present a thorough DKS study of the complete series of alkali aurides, investigating various molecular properties such as dissociation energies, equilibrium bond lengths, harmonic and anharmonic ground-state vibrational constants, and dipole moments. We investigate again the performance of different exchange-correlation functionals and conduct a detailed study of the intermetallic bond by applying several methods which have now been implemented in BERTHA to the analysis of the electron density. In particular, a detailed topological analysis based on the atoms-in-molecules (AIM) theory of Bader[43] has been applied to the relativistic electron density.

II. Theoretical and Computation Details

The formulation of the Dirac−Kohn−Sham scheme implemented in the program BERTHA has been described in a previous article.[42] It was shown that a practical and efficient implementation of the DKS scheme may be constructed following closely the lines of the nonrelativistic theory. In the following, we shall review only some fundamental and peculiar aspects of the theory. The DKS equation, in which only the longitudinal interactions are considered, is given, in atomic units, by

$$\{c\boldsymbol{\alpha}\cdot\mathbf{p} + \beta c^2 + v^{\mathrm{L}}(\mathbf{r})\}\Psi_i(\mathbf{r}) = E_i\Psi_i(\mathbf{r}) \tag{1}$$

where the diagonal potential operator $v^{\mathrm{L}}(\mathbf{r})$ is given by the sum of three terms

$$v^{\mathrm{L}}(\mathbf{r}) = v_{\mathrm{ext}}(\mathbf{r}) + v_{\mathrm{H}}^{\mathrm{L}}[\rho(\mathbf{r})] + v_{\mathrm{xc}}^{\mathrm{L}}[\rho(\mathbf{r})] \tag{2}$$

$v_{\mathrm{ext}}(\mathbf{r})$ represents the external potential due to the fixed nuclei, $v_{\mathrm{H}}^{\mathrm{L}}[\rho(\mathbf{r})]$ represents the electronic Coulomb interaction, which is a functional of the relativistic charge density $\rho(\mathbf{r})$, and the term denoted $v_{\mathrm{xc}}^{\mathrm{L}}[\rho(\mathbf{r})]$ is the relativistic longitudinal exchange-correlation potential, whose exact form is, like that of the corresponding nonrelativistic quantity, unknown. A four-spinor solution of eq 1 is of the form

$$\Psi_i(\mathbf{r}) = \begin{bmatrix} \Psi_i^{(1)}(\mathbf{r}) \\ \Psi_i^{(2)}(\mathbf{r}) \\ \Psi_i^{(3)}(\mathbf{r}) \\ \Psi_i^{(4)}(\mathbf{r}) \end{bmatrix} \tag{3}$$

In our approach, as in the nonrelativistic case, the components of a DKS spinor solution are expanded as a linear combination of atom-centered functions. The four-component formulation of relativistic density functional theory which is implemented in BERTHA uses a Gaussian basis set whose elements are referred to as *G*-spinors.[42] This basis set does not suffer from the variational problems of kinetic balance[44] and retains all the advantages in the evaluation of multicentered integrals which

make Gaussian-type functions the most widely used expansion set in quantum chemistry. The *G*-spinor functions are eigenfunctions of the total (spin−orbit) angular momentum operators j^2 and j_z and of the Johnson−Lippmann fine-structure operator[42] with eigenvalues $\kappa = \pm 1, \pm 2, \pm 3, \ldots$. The explicit form of these functions may be found in refs 40 and 42. In the DKS module of the BERTHA program, an efficient relativistic generalization of the McMurchie−Davidson algorithm[45−47] has been implemented in which the total electron density is expanded directly into an linear combination of real Hermite Gaussian functions (HGTF). Just as is found in the nonrelativistic context, a *G*-spinor representation of the total charge density can readily be expressed as[42]

$$\rho(\mathbf{r}) = \sum_{\alpha,\beta}\sum_{i,j,k} H[\alpha, \beta; i, j, k; \mathbf{r}]H_0[\alpha, \beta; i, j, k] \qquad (4)$$

Here, $H[\alpha, \beta; i, j, k; \mathbf{r}]$ denotes an auxiliary HGTF expansion function, with α identifying the Gaussian exponent and β the local origin of coordinates. The array $H_0[\alpha, \beta; i, j, k]$ is the relativistic analogue of the scalar Hermite density matrix and is defined following Almlöf[48] by

$$H_0[\alpha, \beta; i, j, k] = \sum_{T=L,S}\sum_{\mu\nu} E_0^{TT}[\mu, \nu; i, j, k]D_{\mu\nu}^{TT} \qquad (5)$$

The E_0^{TT} coefficients, which contain the entire spinor structure, are described in refs 45 and 46. In eq 5, $D_{\mu\nu}^{TT}$ denotes an element of the component density matrices $\mathbf{D}^{LL}$ and $\mathbf{D}^{SS}$, where $T = L$ indicates the large component, and $T = S$ the small component. Using this expansion, the costly explicit transformation from the integrals over the HGTF basis to the four-index two-electron set of *G*-spinor integrals is avoided. This approach allows dramatic simplifications[49] when atomic basis functions share their exponents and especially when the contributing spinors correspond to large values of the angular momentum quantum numbers.

The increased cost of a relativistic four-component calculation compared to the corresponding treatment in a nonrelativistic scalar approximation arises mainly because of the increased work involved in the evaluation of the electron density from the spinor amplitudes, the inherent complexity of which propagates into the cost of constructing the matrix representations of the electrostatic interaction operators. The most intensive computational tasks involve the evaluation of the Coulomb and exchange-correlation integrals for the construction, respectively, of the *J* and *K* interaction matrices. Recently, we showed that excellent performance improvements in execution speed and scalability can be achieved by parallelizing both the *J*-matrix and *K*-matrix construction,[40,41] thus expanding significantly the range of applicability of the method.

All the calculations reported in the present work were performed using the four-component DKS method implemented in the parallel version of the BERTHA program[40−42] as summarized above. The nuclei are described by empirically parametrized Gaussian charge distributions, the details of which may be found in ref 42. The large-component *G*-spinor basis sets we used were obtained from the decontraction of a standard nonrelativistic basis set. In particular, we used the cc-pVTZ basis set[50,51] for the lithium and sodium atoms and the 6-311G(2df,-2pd) basis[52] plus s and p diffuse functions (with exponent 0.0047) for potassium. For the rubidium atom, a 20s16p9d *G*-spinor basis set[53] was adopted, together with a small-component basis set generated by the restricted kinetic balance relation.[44] For the gold atom, we used a kinetically balanced 23s18p17d8f basis on which a diffuse s-type function had been included. The details of the gold basis set optimization and a tabulation of the exponents may be found in ref 37. This basis set has already been used with success in molecular calculations.[37,40,54] The calculations have been carried out by employing the following four widely used nonrelativistic density functionals: the simple Dirac−Slater (S) exchange approximation,[55] the Becke 1988 (B88)[56] exchange plus Perdew 1986 (P86)[57] correlation (BP86), the exchange-correlation functional HCTH93,[58] and the Becke 1988 (B88)[56] exchange plus Lee−Yang−Parr (LYP) correlation[59] (BLYP). The first is an example of local density approximation (LDA), while the remaining three are examples of GGA functionals. The implementation of the functionals is, with some minor adaptions, that described in ref 60.

All calculations were carried out with an energy convergence criterion of 1×10^{-7} hartree, and the equilibrium bond length was determined iteratively using a quadratic fit to the energy. The spectroscopic constants (ω_e, $\omega_e x_e$) were obtained by the standard Dunham[61] treatment, based on a sixth-order polynomial fit to seven points distributed at equidistant intervals of 0.1 Å around the minimum. The equilibrium dipole moment μ_e was calculated at the optimized geometry. To avoid open-shell calculations, the covalent dissociation energy was determined by the cycle

$$D_e(\mathrm{MAu}) = D_{\mathrm{ion}} - \mathrm{IP(M)} + \mathrm{EA(Au)} \qquad (6)$$

using the calculated ionic dissociation energy ($D_{\mathrm{ion}} = E(\mathrm{M}^+) + E(\mathrm{Au}^-) - E(\mathrm{MAu}, r_e)$) and accurate experimental values for the ionization potentials and electron affinities.[62,63] An analogous method for the dissociation energy determination has been used with success by different authors.[38,64]

The numerical cubature employed in the calculation of the exchange-correlation matrix elements adopted Becke's atom-centered partitioning scheme.[65] The scheme used to generate the integration grid in BERTHA is detailed in ref 42. We used atomic-centered cells with a radial integration grid divided in three shells. For the atom of gold, for instance, for the inner and middle shells, there were 20 and 11 radial integration points and 26 and 86 angular integration points, respectively; for the outer integration space, we adopted 20 radial points and 434 angular points. Some calculations with a finer integration grid were also performed in order to assess the accuracy of grid employed. As suggested in ref 54, we employed the atomic radii corresponding to the minimum of the electron density along the gold−alkali bonds.

The analysis of the atomic charge population was carried out using three different charge analysis methods: the Mulliken method,[66] Chelp,[67] and an electrostatic fitting method.[68] In the Mulliken method, the charge q_A on an atom A, is defined by the expression

$$q_A = Z_A - \sum_{T}\sum_{\mu\in A}(D^{TT}S^{TT})_{\mu\mu} \qquad (7)$$

where Z_A denotes the atomic number, S^{TT} the overlap matrix over the *G*-spinor basis functions (with $T = L, S$), and D^{TT} the relativistic electron density matrix. The summation over μ is restricted to those *G*-spinors that are centered on the atom A.

In the Chelp (charge from electric potential) method, the atomic and molecular charges are determined by fitting the molecular electrostatic potentials in the region beyond the van der Waals region of the molecular system (at least 3 Å). The least-squares fit of the charges to the electrostatic potential is

TABLE 1: Computed and Experimental Spectroscopic Constants of the Alkali Aurides

	four-component DKS				RECP[a]			
	S	HCTH93	BP86	BLYP	BP86	BLYP	CCSD(T)	exptl[b]
				LiAu				
r_e (Å)	2.27	2.30	2.27	2.27	2.285	2.283	2.270	
ω_e (cm^{-1})	468.1	457.0	479.9	474.5	469	468	464	
$x_e\omega_e$ (cm^{-1})	3.41	2.62	2.91	3.31				
D_e (eV)	3.13	3.07	3.10	3.12	3.00	2.94	2.75	2.91 ± 0.07[c] 2.92[d]
				NaAu				
r_e (Å)	2.59	2.65	2.62	2.61	2.610	2.618	2.607	
ω_e (cm^{-1})	242.3	224.5	244.7	241.5	236	234	242	
$x_e\omega_e$ (cm^{-1})	1.04	0.98	1.32	1.24				
D_e (eV)	2.76	2.54	2.63	2.69	2.52	2.45	2.27	2.64 ± 0.2[e] 2.20 ± 0.13[f]
				KAu				
r_e (Å)	2.85	2.93	2.87	2.90	2.887	2.921	2.969	
ω_e (cm^{-1})	163.4	152.7	164.3	159.9	162	159	158	169[e]
$x_e\omega_e$ (cm^{-1})	0.50	0.32	0.37	0.33				
D_e (eV)	2.87	2.61	2.72	2.74	2.69	2.58	2.24	2.75 ± 0.2[e]
				RbAu				
r_e (Å)	3.06	3.17	3.10	3.14				
ω_e (cm^{-1})	109.6	99.4	109.4	105.9				
$x_e\omega_e$(cm^{-1})	0.23	0.25	0.28	0.28				
D_e (eV)	2.65	2.40	2.50	2.51				2.48 ± 0.03[g]
				CsAu[j]				
r_e (Å)	3.11	3.23	3.15	3.21			3.263[h]	
ω_e (cm^{-1})	96.0	85.3	93.9	90.8			89.4[h]	
$x_e\omega_e$ (cm^{-1})	0.19	0.17	0.18	0.18			0.21[h]	
D_e (eV)	2.85	2.56	2.70	2.64			2.52[h]	2.53 ± 0.03[i]

[a] Relativistic effective core potential calculations of ref 39. [b] The experimental dissociation energies shown are D_0 values rather than D_e. According to our calculations, the difference between the two should range from 0.006 eV for CsAu to 0.03 eV for LiAu. [c] Ref 28. [d] Ref 106. [e] Ref 27. [f] Ref 29. [g] Ref 31. [h] Four-component CCSD(T) of ref 38. [i] Refs 31, 38. [j] The four-component DKS results for CsAu are from Ref 40.

obtained by finding the minimum of the function

$$f(q_1, q_2, ..., q_n) = \sum_{i=1}^{m} [V(\mathbf{r}_i) - E_i(q_1, q_2, ..., q_n)]^2 \qquad (8)$$

for m sampling points. The molecular electrostatic potential $V(\mathbf{r}_i)$ at each point $\mathbf{r}_i$ has the form

$$V(\mathbf{r}_i) = \sum_A \int \frac{\rho_A(\mathbf{r})}{|\mathbf{r}_i - \mathbf{r}|} d\mathbf{r} - \int \frac{\rho(\mathbf{r})}{|\mathbf{r}_i - \mathbf{r}|} d\mathbf{r} \qquad (9)$$

where $\rho_A(\mathbf{r})$ is the spherical Gaussian distribution that models nucleus[42] A, and $\rho(\mathbf{r})$ is the relativistic electron density defined in eq 4. E_i is the monopole approximation of the electrostatic potential at $\mathbf{r}_i$, due to the net atomic charges q_A

$$E_i = \sum_{A=1}^{N} \frac{q_A}{|\mathbf{r}_i - \mathbf{r}_A|} \qquad (10)$$

where N is the number of atoms in the molecule. This method was found to be particularly efficient in providing realistic atomic charges in cases of strong charge transfer.[69]

The electrostatic fitting method is based on a procedure that expands the relativistic electron density in an auxiliary atom-centered basis set. A presentation of the main ideas at the core of relativistic density fitting may be found in ref 49. Its developments and implementation in BERTHA will be described elsewhere.[68] The relativistic density is a real quantity and can be fitted by a linear combination of atom-centered functions using approaches adapted from nonrelativistic techniques. It is natural to assign to each atom the contribution to the total density coming from the functions centered on that nucleus. In this way, an unambiguous definition can be given of effective atomic charges.

The topological analysis of the relativistic electron density has been carried out using the *Mathematica* program,[70] which has been interfaced with BERTHA.

III. Results and Discussions

A. Spectroscopic Constants. In Table 1, we present the computed bond lengths, harmonic and anharmomic vibrational frequencies, and dissociation energies for the alkali aurides MAu (M = Li, Na, K, Rb) using the four-component DKS method implemented in BERTHA. The available experimental data together with previous theoretical results are also presented. Along the alkali metal series, it can be observed that the S functional predicts the strongest bond with, in general, the shortest bond length r_e and the largest dissociation energy. An exception is the LiAu molecule where the results obtained by the S density functional are comparable with those of the GGA calculations. The fact that the local density approximation tends to overestimate the bond strength has been observed also in the nonrelativistic DFT context.[56,71] Considering just the GGA functionals, we notice that the differences in the computed bond lengths among the various functionals are quite small for the lighter molecules, increasing somewhat for the heavier ones but always remaining within about 2% of each other. In their work, Tong and Cheung[39] reported some molecular properties for the MAu molecules (M = Li, Na, K), calculated both at the DFT and CCSD(T) levels, using relativistic effective core potentials (RECP) for gold and potassium. Compared with our DFT calculations using the same correlation functionals (see Table 1), we note that there is very good agreement (within 0.02 Å)

in the bond length predictions. The DKS results also match almost exactly the RECP−CCSD(T) ones, except for a slightly larger deviation in KAu. In the case of CsAu, the deviations between our results and the four-component CCSD(T) ones of ref 38 are also small, and were analyzed in detail in ref 40.

For the harmonic frequencies, ω_e, our computations yield values that are in general just a few wavenumbers higher than those of the previous DFT calculations using the same functionals. By contrast, the GGA HCTH93 functional gives the lowest harmonic frequencies for all aurides. The largest difference is found for the NaAu molecule using the BP86 functional, where our calculations predict a harmonic constant that is 3.6% higher. In the case of KAu, an experimental determination of the harmonic frequency is available,[27] and comparison with the theoretical data shows that all calculations give quite accurate results. Our DKS value using the BP86 exchange-correlation functional agrees with experiment within 7 cm^{-1}.

The anharmonic constants $x_e\omega_e$ are more difficult to compute accurately compared to other spectroscopic quantities, because they depend on the fourth derivative of the potential energy surface with respect the nuclear positions.[72] Fossgaard et al.[54] made a detailed analysis of relative errors on different spectroscopic constants computed by four-component relativistic DFT on a set of diatomic molecules using different nonrelativistic exchange-correlation functionals. They found that the anharmonicity has a greater sensitivity to the numerical integration scheme than do the other spectroscopic quantities, and no clear trend emerges with respect to basis set sensitivity. The difficulties in the accurate determination of the anharmonic constant using DFT are, of course, not peculiar to the relativistic framework.[73−75] It is a general feature of almost all molecular DFT calculations that the exchange-correlation integrals are evaluated numerically, and the details of the procedure, such as the structures of the atomic cubature cells and the error tolerance in the numerical integration scheme, fix the critical limits on the accuracy that can be achieved.[54] Examples of different methodologies have been proposed in the literature.[73,74] Recently,[40] we investigated these methods in detail for the evaluation of the anharmonicity in the case of the CsAu molecule. By performing numerical tests to establish the optimal spacing in the sampling of the energy curve and estimating the accuracy afforded by the integration scheme employed in the computation of the exchange-correlation matrix elements, we showed that stable estimates of the anharmonic constants can also be obtained in the DFT framework. In the present work, we have computed the anharmonic constants for the whole alkali auride series, confirming the numerical stability of our procedure. Except for the lighter molecules, LiAu and NaAu, for which the anharmonic constants are largest, the results appear to be remarkably independent of the exchange-correlation functional used. We note, in addition, that for all molecules the anharmonic correction to the energy of the vibrational ground state is very small, never exceeding 0.5%.

Examination of Table 1 reveals that our four-component DKS calculations using GGA functionals yield dissociation energies D_e in very good agreement with the experimental figures for all the alkali aurides, and that there is no strong dependency on the functional that is used. The largest deviation, which overestimates the experimental value by about 0.2 eV (less than 5 kcal/mol), is found for LiAu. Only in this case are the RECP−DFT estimates of ref 39 in slightly better agreement with experiment. In general, we predict somewhat larger dissociation energies than those obtained using RECP calculations with the same functionals.[39] A direct comparison between the two series of calculations is, however, complicated by the fact that we use two different schemes. Tong and Cheung[39] computed the dissociation energies by taking the difference between the total energy of the molecule at its equilibrium geometry and the energy of the ground state of the separated atoms, while we have used the thermodynamic cycle described in section 2. For KAu, the calculated dissociation energy lies within the experimental uncertainty. For NaAu, there are two appreciably different experimental estimates,[27,29] and our results agree very well with the more recent one of 2.64 eV.[27] Among previous calculations for NaAu, only the RECP−CCSD(T) value of ref 39 is closer to the smaller experimental estimate of 2.20 eV. Inspection of the RECP−CCSD(T) results for the other molecules, however, suggests that the calculations underestimate the dissociation energy by 0.2−0.5 eV. The estimate of the dissociation energy of the RbAu molecule in the gas phase was made by Busse and Weil[31] using Knudsen cell mass spectroscopy results. They measured the equilibrium constants for the reaction that produces RbAu(g) from atoms in the gas phase in the range of temperatures 1551.2−1712.7 K. Using these experimental data and statistical thermodynamic analysis, they calculated the dissociation energy D_0 to be 239 ± 3.0 kJ/mol (2.48 ± 0.03 eV). The appropriate rotational and vibrational partition functions were determined using empirical estimates for the bond length (3.09 Å) and harmonic frequency (151.1 cm^{-1}). Using the same experimental data and procedure, but with our computed values for the internuclear distance and frequency, we obtain estimates of the dissociation energy that depend only weakly on the exchange-correlation function. For the BLYP results, for example, we find that $D_0 = 2.44$ eV, differing only slightly from the experimental value. The same approach has been used in ref 38 in order to obtain the dissociation energy estimate for CsAu reported in Table 1.

As noted above, the quality of the theoretical results obtained, in particular for the dissociation energies, appears to be essentially independent of the exchange-correlation functional used. A more detailed analysis of the results of Table 1 suggests that the HCTH93 functional tends to underestimate slightly the strength of the bond between gold and the alkali metals, yielding longer bond lengths, smaller harmonic frequencies, and smaller dissociation energies than the other GGA functionals.

B. Electronic Structure and Bonding. The chemical bond between gold and alkali metals in the gas phase is strongly polar, with a significant electron transfer from the alkali metal to the gold atom reinforcing the bond. The extent of the charge transfer may have great importance for the electric properties in the solid state. Scheuring et al. estimated the ionic contribution to the bond using empirical data.[32] Tong and Cheung also predicted a very polarized bond[39] resulting in a very large dipole moment and effective nuclear charge. A population analysis for the CsAu molecule has been carried out by Fossgaard et al.[38] They analyzed in great detail the four-component relativistic Hartree−Fock wave function, using both the Mulliken population and projection methods. The two methods were found to be in qualitative agreement, predicting electron transfer values of 0.96 and 0.71, respectively. These authors emphasized that both relativity and the lanthanide contraction play important roles in describing the polarity of the molecular bond in these systems.

To investigate the extent of the charge transfer and the details of the intermetallic bonding along the whole alkali auride series, we also performed an extensive analysis of the charge distribution using several methods. In addition, we report here a detailed analysis of the electron density based on the topological analysis of Bader.[43]

TABLE 2: Dipole Moments μ (D) and Atomic Charges (excess electrons on Au) for the Alkali Aurides[a]

	four-component DKS				RECP[b]		
	S	HCTH93	BP86	BLYP	BP86	BLYP	CCSD(T)
				LiAu			
μ	5.8	6.0	5.9	6.0	6.26	6.08	5.19
Z_{eff}	0.54	0.55	0.54	0.55	0.58	0.56	0.48
Mulliken	0.05	0.07	0.05	0.08			
Fitting	0.70	0.70	0.71	0.71			
Chelp	0.74	0.75	0.76	0.76			
				NaAu			
μ	7.1	7.5	7.3	7.1	7.50	7.05	6.48
Z_{eff}	0.57	0.59	0.58	0.56	0.60	0.57	0.52
Mulliken	0.34	0.43	0.35	0.34			
Fitting	0.73	0.74	0.74	0.78			
Chelp	0.77	0.78	0.78	0.79			
				KAu			
μ	8.9	9.5	9.3	9.2	9.43	9.12	9.36
Z_{eff}	0.65	0.67	0.67	0.66	0.69	0.66	0.66
Mulliken	0.67	0.72	0.67	0.70			
Fitting	0.85	0.87	0.85	0.86			
Chelp	0.92	0.90	0.90	0.90			
				RbAu			
μ	10.4	10.5	10.3	10.7			
Z_{eff}	0.71	0.69	0.70	0.71			
Mulliken	0.83	0.79	0.81	0.83			
Fitting	0.86	0.83	0.84	0.86			
Chelp	0.89	0.89	0.89	0.87			
				CsAu[d]			
μ	9.9	10.8	10.2	10.7			11.73[c]
Z_{eff}	0.66	0.70	0.67	0.69			0.75[c]
Mulliken[e]	0.99	0.93	1.05	1.01			
Fitting	0.93	0.93	0.93	0.94			
Chelp	0.96	0.97	0.98	0.97			

[a] The charges are computed using Mulliken analysis, the fitting method, and the Chelp method (see text). The effective nuclear charge Z_{eff} is obtained as the dipole moment divided by the internuclear distance. [b] Relativistic effective core potential calculations of ref 39. [c] Four-component CCSD(T) of ref 38. [d] The four-component DKS results for CsAu are from ref 40. [e] The relativistic Hartree−Fock Mulliken charge for CsAu is computed to be 0.96 in ref 38.

1. Dipole Moment and Charge Transfer. In Table 2, we report the computed dipole moments and charges for the alkali auride molecules, together with previously available results. Our calculations consistently confirm the very large dipole moments found by Tong and Cheung.[39] For the RbAu molecule, we found a dipole moment that is in the range of 10.3 D (BP86) to 10.7 D (BLYP), a value that is similar to that obtained for CsAu.[40] While the exchange-correlation functionals we have used apparently all give very similar results for the dipole moment, the trend of DFT results compared with CCSD(T) is unclear. For LiAu and NaAu, the DFT calculations give larger dipole moments than CCSD(T). For KAu, the two methods essentially give equivalent results, while for the heavier CsAu, the dipole moments calculated using DFT are smaller than the CCSD(T) values by 1−2 D. The exact cause of this pattern is difficult to establish. While the DFT formalism has proven to be a successful approach to the calculation of dipole moments in small and light molecules,[54,76] studies of the performance of DFT models for the calculation of dipole moments of molecular systems containing heavy atoms are more scarce. Already for a system such as CuCl, the DFT results were rather disappointing.[77] Obviously, in a molecule with atoms of high atomic number, small changes in the nuclear positions, even within the uncertainty in the computed equilibrium positions, may cause significant variations in the dipole moment.

The atomic charges shown in Table 2 have been computed using different population analysis methods: besides the Mulliken charges, also the Chelp and the electrostatic fitting methods described in section 2. We also report the values of the effective charge Z_{eff}, which is the effective value of the point charge transferred which would give rise to the computed dipole moments at the equilibrium internuclear distance. Z_{eff} takes into account no polarization effects and so provides a lower limit to the amount of electronic charge transferred. As with the dipole moments, the computed charges show remarkably little dependence on the exchange-correlation functional used. The computed electron transfer from the alkali metal to gold increases as the nuclear charge of the alkali atom is increased from Li to Cs. However, while all the charge analysis methods give comparable results for the heavier molecules, the Mulliken charges differ strikingly from the other approaches for the light element systems, even predicting an essentially neutral LiAu. For CsAu, the results we obtain using DFT orbitals are close to the charge transfer of 0.96 reported by Fossgaard et al. by analysis of a relativistic Hartree−Fock wave function.[38] It is well-known that the Mulliken charges are strongly dependent on the basis set, and in addition, they are particularly unreliable when heavy atoms are involved because the overlap charge may be large. Indeed, we find large Mulliken overlap charges for LiAu and NaAu (0.47 and 0.30, respectively, with the BLYP functional), while they drop to 0.19 for KAu and 0.03 for RbAu and become negative (−0.38) for CsAu. Szefczyk et al.[69] compared several population analysis methods using various theoretical approaches and basis sets. They concluded that the Chelp approach gives the best performance in terms of computed charge transfer values, with the advantage that the results converge rapidly with the basis set. In our series of molecules, the Chelp and electrostatic fitting methods give consistently similar results, with the Chelp figures systematically slightly larger. In LiAu and NaAu, the alkali atomic charges are 0.70−0.76 and 0.73−0.79, respectively. KAu and RbAu turn out to have very similar charge transfers of roughly 0.9 electrons, with a somewhat larger value obtained for CsAu. The results reflect the trend in the computed effective charges.

2. Topological Analysis of the Electron Density. The topological analysis of the electron density, developed in the framework of the theory of atoms in molecules (AIM) of Bader et al.,[43] has been applied widely to study several chemical properties of small molecules such as the nature of chemical bonding, molecular stability, and chemical reactivity.[78] It has subsequently also been applied to molecules containing transition metals,[79−85] and a very recent example is the work of Müller-Rösing et al.[86] on the silver−silver bond in the silver halides. Some investigations have also been conducted on molecules and clusters containing gold.[87−89] To our knowledge, however, Bader's topological analysis has not previously been applied to fully relativistic electron densities of molecules.

For molecular systems composed of light atoms, the topological analysis of the electron density is known to give results in good agreement with experiment.[90] On the other hand, the study of the topological properties of the electron density presents some difficulties, both in experiments and in calculations, when heavy atoms are involved and, especially, if relativistic effects are taken into account. In diffraction experiments aimed at the determination of the electron density, the large number of core electrons of heavy atoms may cause loss of accuracy (see ref 91 and references therein). From the theoretical point of view, the topological analysis of the density for a molecular system containing heavy atoms may be especially problematical, particularly near the nuclei, due to the use of effective core potentials and the consequent absence of an explicitly repre-

TABLE 3: Topological Analysis (DKS/BLYP) of the Electron Density for the Alkali Aurides and Au_2[a]

	r_b	$\rho(\mathbf{r}_b)$	$\nabla^2\rho(\mathbf{r}_b)$	$\lambda_{1,2}$	λ_3	$G(\mathbf{r}_b)$	$H(\mathbf{r}_b)$	$G(\mathbf{r}_b)/\rho(\mathbf{r}_b)$
LiAu	1.529	0.0348	0.1521	−0.0396	0.2315	0.0360	0.0020	1.034
NaAu	1.573	0.0268	0.1178	−0.0235	0.1649	0.0265	0.0029	0.989
KAu	1.574	0.0270	0.0887	−0.0204	0.1295	0.0218	0.0004	0.807
RbAu	1.653	0.0200	0.0671	−0.0127	0.0927	0.0154	0.0014	0.770
CsAu	1.622	0.0232	0.0652	−0.0143	0.0938	0.0162	0.00002	0.670
Au2	1.244	0.0831	0.1997	−0.0729	0.3456	0.0787	−0.0287	0.947

[a] Distance r_b (Å) of the bond critical point from the gold atom, electron density $\rho(\mathbf{r}_b)$ (e/(au)^3) at the bond critical point, Laplacian $\nabla^2\rho(\mathbf{r}_b)$ (e/(au)^5) at the bcp, eigenvalues of the Hessian of the electron density along the interatomic axis (λ_3) and along the perpendicular directions ($\lambda_{1,2}$), the kinetic energy density $G(\mathbf{r}_b)$ (hartree/(au)^3), total energy density $H(\mathbf{r}_b)$ (hartree/(au)^3) and the kinetic energy per electron $G(\mathbf{r}_b)/\rho(\mathbf{r}_b)$ (hartree/e).

sented core electron density.[92] Some of these problems may be overcome if one adds a posteriori the core−electron density obtained by atomic calculations.[93] When relativistic effects are important, global topological properties of the electron density can be predicted reliably only by fully relativistic calculations. Numerical studies[94] on atoms indicate that, in order to describe accurately the density topology in the valence region, the number of core electrons simulated by relativistic core potentials must be small. In the present work, all our topological analysis has been based on the relativistic electron density obtained by all-electron DKS calculations. This will give us the advantage of correctly tracking the relativistic effects and analyzing electron densities that are not affected by the use of relativistic effective core potentials.

We recall that the topological analysis of the density consists principally of the search of the critical points (cps) of the three-dimensional function $\rho(\mathbf{r})$, defined as the points where the gradient field $\nabla\rho(\mathbf{r})$ vanishes. The cps are characterized by the three eigenvalues (λ_1, λ_2, λ_3) of the Hessian matrix of $\rho(\mathbf{r})$ and are labeled as (r, s) according to their rank, r, which is the number of nonzero eigenvalues, and their signature, s, which is defined to be the algebraic sum of the signs of the eigenvalues. There are thus four types of stable cps for $r = 3$. In particular, we are here concerned with the so-called bond critical points (bcp), characterized as having two negative and one positive Hessian eigenvalues. A bcp $\mathbf{r}_b$ is therefore a maximum in the plane defined by the two Hessian eigenvectors corresponding to the negative eigenvalues and a minimum along the third perpendicular eigenvector direction. A chemical bond between two nuclei is then characterized by a line of maximum electron density which links two atomic nuclei and intersects the zero-flux surface separating the two nuclear basins at a bcp.

In Table 3, we report the main topological parameters computed with the BLYP functional for the alkali aurides. Some test calculations employing the other GGA functionals have been performed, and the results do not differ appreciably from those obtained using the BLYP functional. In the topological analysis, it is useful to have a comparative approach[91] in which topological quantities may be related to the chemical interactions. To this purpose, we have also carried out calculations on Au_2. The first parameter reported in the table is the distance from gold of the bond critical point located at the intersection of the line joining the nuclei with the zero flux surface. It should be noted that, as expected for diatomic molecules, the electron density does not exhibit any other bcp. For these highly symmetric molecules, the position of the bcp may be taken as a measure of the atomic dimensions in the molecule. The homonuclear case of Au_2, where by symmetry the bcp lies exactly in the middle of the bond, represents a useful reference. As can be seen in the Table, the bcp of the alkali aurides all lie significantly farther away from the gold atom than from the alkali atom and in a narrow range of values between 1.529 and 1.653 Å. This is particularly striking when viewed in comparison to the bond distances between gold and the alkali atoms which, on the contrary, vary widely (from 2.27 to 3.21 Å) along the series. This is a clear indication that the size of the gold atom in the alkali auride molecules is both fairly independent of the alkali metal and much bigger than in the gold dimer, reflecting accurately the ionic character of the bond. Note, in particular, that the ratio of the gold atomic volumes implied by the r_b values and the corresponding Chelp charges (Table 2) is roughly constant along the series.

The ionicity of the alkali aurides is also confirmed by the very small value of the electron density at the bond critical point, reported in Table 3. Such small values are typical of ionic molecules such as NaBr and NaI that have $\rho(\mathbf{r}_b)$ values of 0.0316 and 0.0265 e/au^3, respectively (see below). In contrast, the Au_2 molecule presents an electron density at the bond critical point that is nearly three times as large as for the alkali aurides, reflecting a greater accumulation of the electron density in the internuclear zone.

The Hessian of the electron density at the bond critical points has some special features that permit a topological description of the chemical bond. We recall that the Hessian at the bcp has one positive eigenvalue and two negative eigenvalues. In diatomic molecules, the density curvature at r_b along the internuclear axis, λ_3, is the positive value, implying that the charge density is locally depleted at the bcp along this direction. Consequently, the two perpendicular curvatures $\lambda_{1,2}$, which are equal by symmetry, are now negative: In these directions, the density has a maximum at r_b. So, from a topological point of view, the formation of a chemical bond and its associated interatomic surface is the result of the perpendicular accumulation of density toward the internuclear line and the parallel flow of density away from the zero-flux surface, leading to its separate concentration in each of the atomic basins. The dominant effect may be described qualitatively by the sign of the Laplacian of the density (the trace of the Hessian matrix) $\nabla^2\rho(\mathbf{r}_b)$ at the bond critical point.[78] For the molecular systems studied here, the positive eigenvalue λ_3 dominates, so that the Laplacian of the electron density at the bcp is positive. It has to be noted, however, that the Hessian eigenvalues are very small at the bcp, both in the internuclear direction and perpendicular to it. Such flat density in the interatomic region was found to be a peculiar, but general, feature of the metallic bond.[79]

The relationship between the sign and magnitude of the Laplacian and the nature of the electronic structure has been studied in detail, both for atoms and for molecules.[78] Its particular strength is that it maps the regions in which the electron density is concentrated or depleted. Where the Laplacian of the electron density has a negative sign, the electron density is locally concentrated, and conversely, if the Laplacian is positive, the electron density is locally depleted. At the atomic level, the analysis of the Laplacian density reveals a spherical symmetry with alternating signs that start with negative values on the nuclei. These alternating signs define a Laplacian shell structure, where each shell is characterized by a negative Laplacian and is separated from the next by a positive region. For light atoms, a strict correspondence has been observed between the shell structure of the Laplacian and the electron shell structure,[78,94−96] but for the heavier atoms, this correspondence is not so strictly observed and may even be lost

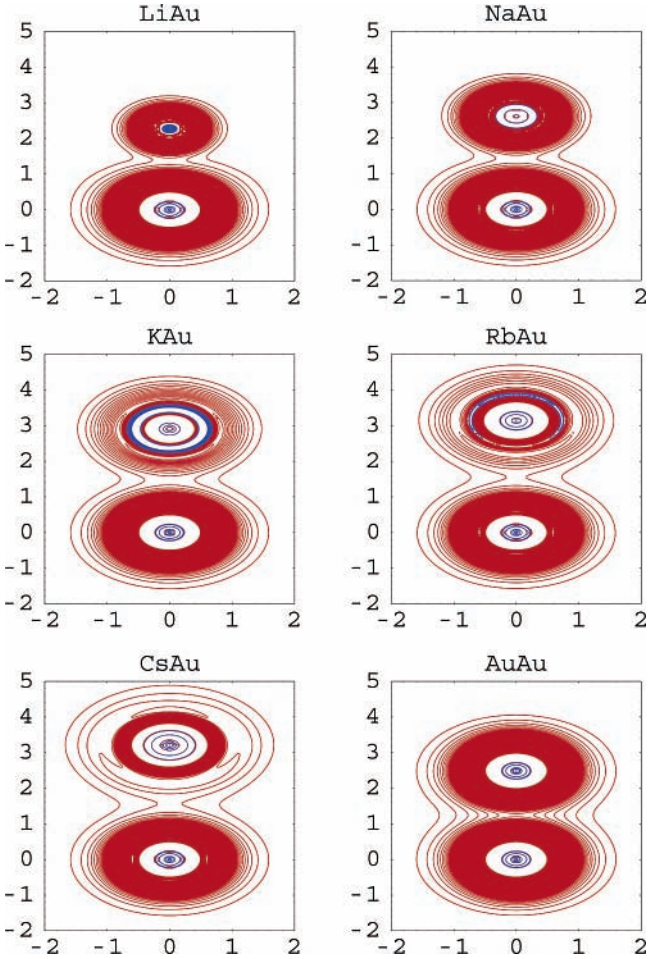

Figure 1. Contour plots of the Laplacian of the electron density (in e/(au)^5) for the alkali aurides and the gold dimer. The positive contour levels (red) range from 0.03 to 10.00 with step 0.03, while the negative ones (blue) from 0 to −7000 with step 10. Distances are in Å.

entirely for the outer valence shells.[80,97,98] For example, numerical result of Kohout et al.[94] indicates that the Laplacian of Au^- exhibits only four shells. We have confirmed this in detail in our own DKS calculations and analysis of the average electronic shell radii. The results of this analysis are available as Supporting Information.

For light-atom molecules, the Laplacian shell structure is found to persist, and its features, in particular, its sign at the bcp, change according to the nature of the chemical bond. For example, ionic bonds, hydrogen bonds, and van der Waals interactions are typically found to be associated with a positive sign of the Laplacian at the bcp, while covalent bonds are more often associated with a negative sign of the Laplacian at the bcp.[78] These correspondence rules have met with some success in describing the chemical interactions in molecules containing first- and second-row atoms but are found to be much more uncertain, or to fail completely, when atoms heavier than those of the third row are involved.[91] This failure is clearly related to the loss of the atomic valence shell structure of the Laplacian discussed above and is confirmed also for the molecules we have studied in this work. We found positive values of the Laplacian of the electron density for all molecules, not only the stongly ionic alkali aurides but also the homonuclear species Au_2. In fact, the Laplacian value at the bcp of Au_2 is greater than that of the alkali aurides.

In Figure 1, we display the contour plots of the Laplacian electron density and in Figure 2 the plots of its value on a plane

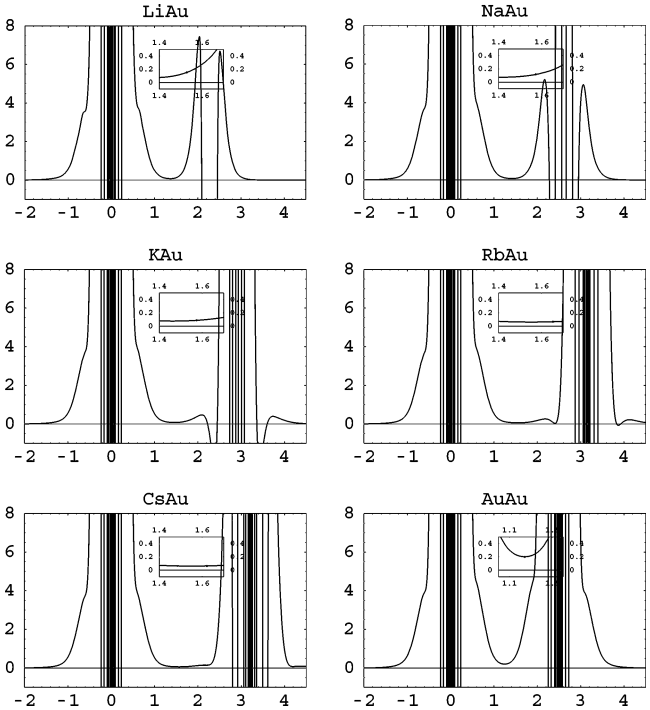

Figure 2. Cut of the Laplacian electron density (in e/(au)^5) along the internuclear axis for the alkali aurides and the gold dimer. Distances are in Å.

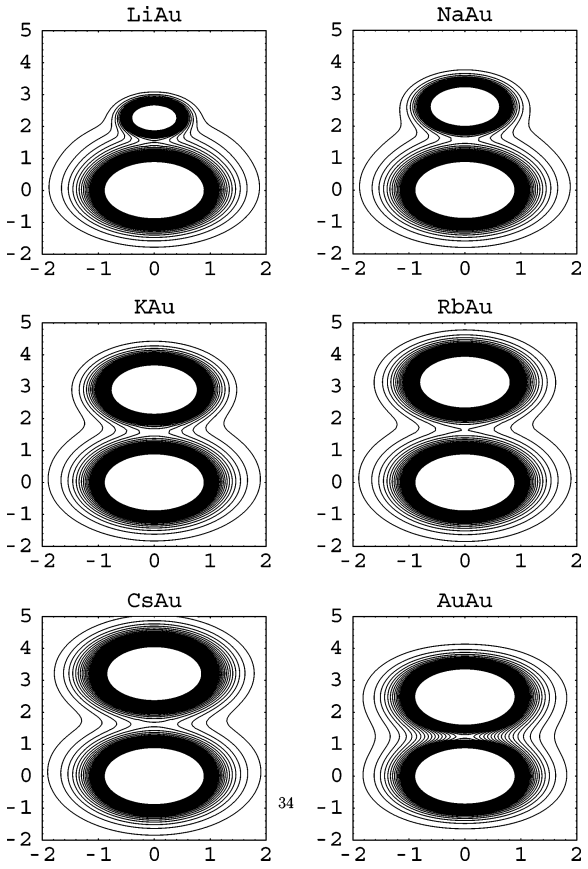

Figure 3. Contour plots of the electron density (e/(au)^3) from 0.005 to 0.2 with step 0.005 for the alkali aurides and Au_2. Distances are in Å.

containing the nuclei. In Figure 3, we display the contour plots of the electron density itself. By inspection of Figure 1 and Figure 3, the most eye-catching feature is that the Laplacian plots are much more structured than the electron density plots,

and they differ strongly from molecule to molecule, providing a sort of "molecular fingerprint". All molecules are characterized by positive values of the Laplacian over a wide internuclear region. The alkali aurides present values of the Laplacian at the bcp that are very small and decrease progressively on passing from LiAu to CsAu. For these molecules, the Laplacian profile in the region of the bcp is rather flat and becomes flatter along the series (see Figure 2). By contrast, the bcp in Au_2 is found in a region of the Laplacian profile with a higher curvature.

The contour plots in Figure 1 show clearly the atomic inner shell structure of the Laplacian, with the alternating sign displayed as a change in color. Considering first the shell structure of the alkali metals in the smallest aurides LiAu and NaAu, we clearly identify one and two shells. In the isolated atoms, one more outermost shell is observed, which disappears in the ionic aurides due to the electron transfer from the alkali metal to gold. In KAu, a similar situation is observed, with three shells surrounding the potassium. However, in this case, the absence of a fourth shell may already be a consequence of the loss of atomic Laplacian structure discussed above for heavy atoms. In this connection, we recall that the Laplacian was found to be positive at the bcp of the homonuclear K_2 system, while it is negative for Na_2.[91]

The heavy-atom features of the Laplacian become evident for RbAu. Atomic rubidium already lacks the outermost (fifth) shell of the Laplacian, so that the charge transfer to gold is not visible. Interestingly, however, the fourth atomic shell is clearly altered upon formation of the chemical bond with Au. In the direction away from Au, the shell remains evident (negative sign), but it disappears in the direction toward the gold atom (positive sign). In the case of CsAu, the fifth electron shell (5s, 5p, 5d) is not represented at all in the Laplacian shell structure.

Besides the Laplacian, an important local quantity that has been considered in the description and characterization of the chemical bond is the total energy density at the bcp.[100,101] The total energy density $H(\mathbf{r})$ is defined as the sum of the kinetic energy density $G(\mathbf{r})$ (positive definite) and the potential energy density $V(\mathbf{r})$ (negative). It is typically found that the total energy density is positive (i.e., the kinetic energy density dominates) in regions from which the electron density tends to escape, whereas $V(\mathbf{r})$ dominates in regions in which the electron density is bound.[78] For covalent bonds in small molecules, $H(\mathbf{r})$ at the bcp is typically negative,[100] while it is positive for ionic bonds or on the interatomic surface separating two noble gas atoms.[102] In contrast to the properties of the Laplacian shell structure, these features of the energy density tend to be preserved also when heavy atoms are involved.[91]

We have computed the energy densities of the alkali aurides at the bcp as reported in Table 3. The density of kinetic energy has been determined using two different approaches. In the first, we have applied the semiempirical functional form proposed by Abramov,[103] which relates the kinetic energy density to the electron density and its Laplacian at the bcp. This approach is often used to estimate the kinetic energy density from the topological analysis of the experimental electron density without the necessity of a molecular wave function.[104] In the second approach, we have calculated $G(\mathbf{r})$ using the definition of the relativistic (positive definite) kinetic energy operator and our spinor solutions of the DKS equation, according to the following expression

$$G(\mathbf{r}) = \sum_a \Psi_a^{\dagger}(\mathbf{r})\{c\boldsymbol{\alpha}\cdot\mathbf{p} + \beta c^2 - \mathbf{I}c^2\}\Psi_a(\mathbf{r}) \qquad (11)$$

where the sum is extended to the occupied electronic states. Of course, identifying this expression with the kinetic energy density implies the widely used approximation of using DFT orbitals as electronic wave functions and the formal division of the total electronic energy into electrostatic, kinetic, and rest-mass contributions. We show in the table only the former results, because the two approaches provide virtually identical values for the alkali aurides. We note here, however, that eq 11 gives a somewhat smaller kinetic energy density for Au_2 (0.0671 hartree/bohr^3) than that reported in the table. Remarkably, all alkali aurides bonds are characterized by positive values of the total electron energy density, $H(\mathbf{r}_b)$ at the bcp, as is expected in ionic bonds.[91] It should also be noted, however, that the values are generally very small and, in fact, almost vanishingly small for CsAu. For the Au_2 molecule, $H(\mathbf{r}_b)$ instead adopts a negative value of large magnitude. The potential energy contribution here dominates, which is typical of covalent bonds. We see therefore that, for these systems containing heavy atoms, the analysis of the Laplacian shell structure fails to characterize the chemical bond, while the energy density analysis still appears to discriminate between ionic and covalent bonding. The generality of these conclusions is, however, not yet established and requires further study, as is indicated by the tiny bcp energy density for the alkali aurides and the restriction of all of our test systems to those involving metal−metal bonds.

In Table 3, we finally report the quantity $G(\mathbf{r}_b)/\rho(\mathbf{r}_b)$, which may be called the kinetic energy per electron.[78] Usually, it is in excess of unity for ionic interactions, while it is less than unity for covalent bonds (see refs 91 and 102). For our molecular systems, however, we do not find this kind of simple relation. With the exception of the LiAu molecule, the values of $G(\mathbf{r}_b)/\rho(\mathbf{r}_b)$ are smaller than unity both for the alkali aurides and for Au_2. Thus, the $G(\mathbf{r}_b)/\rho(\mathbf{r}_b)$ quantity does not seem to be particularly useful in characterizing the chemical bond for the heavy-atom molecules discussed here.

3. The Topological Similarity between Gold and the Halogens (Br, I). As a final issue, we would like to discuss the analogy between gold and the halogens from a topological point of view. The suggestion that gold should be regarded as possessing the chemical properties of a halogen is certainly fascinating and has been explored in a recent review by Pyykkö.[14] Gagliardi,[11] predicting the stability of uranium tetraauride, has investigated some different metal tetraauride compounds, in which gold acts as a ligand to the metallic center with a formal charge of −1. It was shown that $ThAu_4$ and UAu_4 present bond lengths which are intermediate between the corresponding bromides and iodides. On the basis of this idea, we have investigated possible similarities between gold and the halogens in the series of respective compounds with the alkali metals. In Table 4, we reconsider the main topological parameters for the alkali aurides together with those of the corresponding halides (Br, I). The latter were also computed by us based on the relativistic electron density obtained by DKS/BLYP computations. The large-component *G*-spinor basis sets for Br and I were obtained by decontracting the 6-311G** basis sets.[105,106] The equilibrium bond length and the dissociation energy shown in the table for the alkali bromides and iodides are the experimental values.[107] The bond length of the aurides obtained in these studies are systematically intermediate between those of the two corresponding halides, confirming the analogous findings of ref 11 mentioned above. Remarkably, these results appear to be independent of the exchange-correlation functional employed for the calculation of the bond length in the alkali aurides.

Turning now to the results of the topological analysis, it is surprising that, except in the case of RbAu, all topological

TABLE 4: Comparison of the Topological Properties of the Electron Density for the Alkali Aurides and Halides[g]

	r_e	r_b	$\rho(\mathbf{r}_b)$	$\nabla^2\rho(\mathbf{r}_b)$	$\lambda_{1,2}$	λ_3	$G(\mathbf{r}_b)$	$H(\mathbf{r}_b)$	D_0
LiBr	2.022[a]	0.678	0.0537	0.2633	−0.0750	0.4133	0.0658	0.00001	4.45[a]
LiAu	2.27[b]	0.741	0.0348	0.1521	−0.0396	0.2315	0.0360	0.0020	2.91[c]
LiI	2.392[a]	0.751	0.0330	0.1258	−0.0355	0.1969	0.0307	0.0007	3.57[a]
NaBr	2.502[a]	1.010	0.0316	0.1453	−0.0309	0.2071	0.0333	0.0030	3.8[a]
NaAu	2.61[b]	1.037	0.0268	0.1178	−0.0235	0.1649	0.0265	0.0029	2.64[d]
NaI	2.711[a]	1.048	0.0265	0.1015	−0.0219	0.1452	0.0237	0.0017	3.05[a]
KBr	2.821[a]	1.303	0.0292	0.0994	−0.0235	0.1466	0.0245	0.0003	3.94[a]
KAu	2.90[b]	1.326	0.0270	0.0887	−0.0204	0.1295	0.0218	0.0004	2.75[d]
KI	3.048[a]	1.354	0.0242	0.0709	−0.0168	0.1046	0.0176	0.00001	3.4[a]
RbBr	2.945[a]	1.413	0.0259	0.0953	−0.0187	0.1328	0.0223	0.0014	4.0[a]
RbAu	3.14[b]	1.487	0.0200	0.0671	−0.0127	0.0927	0.0154	0.0014	2.48[e]
RbI	3.177[a]	1.469	0.0214	0.0694	−0.0135	0.0966	0.0163	0.0010	3.47[a]
CsBr	3.072[a]	1.534	0.0260	0.0797	−0.0195	0.1188	0.0198	0.0001	4.07[a]
CsAu	3.21[b]	1.588	0.0232	0.0652	−0.0143	0.0938	0.0162	0.00002	2.53[f]
CsI	3.315[a]	1.602	0.0214	0.0589	−0.0137	0.0862	0.0145	0.0002	3.4[a]

[a] Ref 106. [b] This work DKS/BLYP. [c] Ref 28. [d] Ref 27. [e] Ref 31. [f] Refs 31, 38. [g] The parameter r_e is the equilibrium bond length (Å); the other terms are as in Table 3, except that the bond critical point, r_b, is here defined as distance from the alkali metal. The experimental dissociation energies D_0 (eV) are also shown.

parameters for the alkali aurides again fall between those of the bromides and iodides. Only the total electron energy density at the bcp does not show such a trend, but this parameter is extremely small for all molecules. For the rubidium compounds, the order of the auride and iodide topological parameters is inverted, so that the parameters of RbI are found to lie between those of RbBr and RbAu. It should be noted, however, that the auride and iodide parameters are always very close to each other in the rubidium case.

Despite the surprising similarities between the alkali halides (Br and I) and aurides, in terms of both the bond lengths and the topology of the electron density, the energetics are quite different. In particular, the dissociation energy of the aurides is smaller than for the corresponding halides. Furthermore, the alkali aurides have a different behavior than the halides in the solid state. For instance, while the halides are typically insulators, the aurides of lithium, sodium, and potassium are metallic solids, while the aurides of rubidium and cesium are semiconductors. CsAu and RbAu crystallize in the octacoordinated CsCl stucture, as do all other cesium halides. The halides of the other alkali metals have a NaCl structure, but the structures of the metallic NaAu and KAu have not yet been fully elucidated. More than one structure appears to have been observed for LiAu.[18]

Conclusions

The spectroscopic properties and the electronic structure of the groud state of the complete series of alkali aurides have been investigated within the four-component formulation of relativistic density-functional theory recently implemented in the BERTHA program. For the RbAu molecule, this has represented the first theoretical study that attempts to predict its molecular properties. The nature of the intermetallic bond of the alkali aurides has been investigated in terms of both dipole moments and charge transfer and the topological analysis of the fully relativistic electron density.

The present study has confirmed that a model constructed using a detailed four-component treatment of the Dirac−Kohn−Sham amplitudes expanded in a *G*-spinor basis set correctly recovers one-body relativistic corrections. It has also demonstrated that the use of the available nonrelativistic gradient-corrected density functionals in conjunction with a density derived from these relativistic amplitudes yields results whose quality is comparable to what one would expect in nonrelativistic quantum chemical studies. The largest deviation from the experimental value of the dissociation energies in the alkali aurides has been found to be about 0.2 eV (less than 5 kcal/mol). Such accuracies are fully within the limits expected of GGA functionals. The nonrelativistic GGA functionals used have given results that are close to each other. The HCTH93 functional tends to underestimate slightly the strength of the bond between gold and the alkali metals.

The molecules studied have large dipole moments that increase as nuclear charge is increased within a series. A significant electron transfer from the alkali metals to gold has been observed. We have used several methods to analyze the charge density. The Mulliken charge analysis fails to describe the charge transfer for the lighter alkali aurides because of the large overlap charge. The most reliable data on charge transfer appear to be those obtained by the Chelp method.

In the present study, we have, for the first time, used a fully relativistic electron density obtained by four-component density functional theory to carry out a detailed topological study of molecular electron density distributions. The comparative study of the topological properties of the alkali aurides, together with those of the gold dimer, have confirmed the strong ionicity in the alkali aurides. By studying the Laplacian of the electron density, it has been confirmed that the outer valence shells in the Laplacian structure may be lost entirely for heavy atoms. A detailed study of the Laplacian shell structure of the Au^- ion has shown that only four shells are formed, and that they correlate strongly with the first four electronic shells. For molecules containing heavy atoms such as the ones studied here, the analysis of the sign of the Laplacian at the bond critical point fails to characterize correctly the chemical bond, while the energy density analysis appears to provide accurate discrimination between ionic and covalent bonding. The generality of these conclusions calls however for further study. The bond between gold and the alkali metals presents several similarities with the alkali halides. For several molecular properties, including bond lengths and the main parameters characterizing the density topology, almost all the aurides are intermediate between the corresponding bromides and iodides.

In many cases, there are no experimental data with which we are able to compare the spectroscopic and electronic properties that we have obtained theoretically for the alkali aurides. Experimental work to resolve the rotational structure of the alkali aurides would provide very interesting data against which to test our theoretical predictions. Furthermore, these molecules provide examples of very stable metal−metal bonds

in systems that exhibit unusually large dipole moments and appear to be suitable candidates for studies of Fourier transform microwave spectroscopy.

Supporting Information Available: Details of the Laplacian shell structure obtained by our DKS calculations for Au^- and analysis of the average electronic shell radii. This material is available free of charge via the Internet at http://pubs.acs.org.

References and Notes

(1) Alexeev, O. S.; Gates, B. C. *Ind. Eng. Chem. Res.* **2003**, *42*, 1571.
(2) Leonard, R. M.; Bhuvanesh, N. S. P.; Schaak, R. E. *J. Am. Chem. Soc.* **2005**, *127*, 7326.
(3) Gingerich, K. A. In *Current Topics in Meterials Science*; Kaldis E., Ed.; North-Holland: New York, 1980.
(4) Schwerdtfeger, P.; Dolg, M. *Phys. Rev. A* **1991**, *43*, 1644.
(5) Balducci, G.; Ciccioli, A.; Gigli, G. *J. Chem. Phys.* **2004**, *121*, 7748.
(6) Heinebrodt, M.; Malinowski, N.; Tast, F.; Branz, W.; Billas, I. M. L.; Marlin, T. P. *J. Chem. Phys.* **1999**, *110*, 9915.
(7) Tanaka, H.; Neukermans, S.; Janssens, E.; Silverans, R. E.; Lievens, P. *J. Chem. Phys.* **2003**, *119*, 7115.
(8) Heiz, U.; Vayloyan, A.; Schumacher, E.; Yeretzian, C.; Stener, M.; Gisdakis, P.; Rösch, N. *J. Chem. Phys.* **1996**, *105*, 5574.
(9) Pyykkö, P. *Chem. Rev.* **1988**, *88*, 563.
(10) Schwerdtfeger, P. *Angew. Chem., Int. Ed.* **2003**, *42*, 1892.
(11) Gagliardi, L. *J. Am. Chem. Soc.* **2003**, *125*, 7504−7505.
(12) Zhao, Y.; Pérez-Segarra, W.; Shi, Q.; Weil, A. *J. Am. Chem. Soc.* **2005**, *127*, 7328.
(13) Mendizabal, F.; Pyykkö, P. *Phys. Chem. Chem. Phys.* **2004**, *6*, 900−905.
(14) Pyykkö, P. *Angew. Chem., Int. Ed.* **2004**, *43*, 4412−4456.
(15) Sommer, H. *Nature (London)* **1943**, *152*, 215.
(16) Spicer, W. E.; Sommer, A. H.; White, J. G. *Phys. Rev.* **1959**, *115*, 57.
(17) Zachwieja, U. *Z. Anorg. Allg. Chem.* **1993**, *619*, 1095.
(18) Grosch, G. H.; Range, K.-J. *J. Alloys Compd.* **1996**, *233*, 30.
(19) Koenig, C.; Christensen, N. E.; Kollar, J. *Phys. Rev. B* **1983**, *29*, 6481.
(20) Christensen, N. E.; Kollar, J. *Solid State Commun.* **1983**, *46*, 727.
(21) Watson, R. E.; Weinert, M. *Phys. Rev. B* **1993**,*49*, 7148.
(22) Pyykkö, P. *Angew. Chem., Int. Ed.* **2002**, *41*, 3573.
(23) Pelton, A. D. *Bull. of Alloy Phase Diagrams* **1986**, *7*, 19.
(24) Costa Gabral, B. J.; Silva Fernandes, F. M. S. *AIP Conf. Proc.* **1995**, *330*, 129−133.
(25) Matsunaga, S. *J. Phys. Soc. Jpn.* **2000**, *69*, 1712−1716.
(26) Mudring, A.; Jansen, M.; Daniels, J.; Krämer, S.; Mehring, M.; Ramalho, J. P. P.; Romero, A. H.; Parrinello, M. *Angew. Chem.* **2002**, *114*, 128.
(27) Stangassinger, A.; Knight, A. M.; Ducan, M. A. *J. Phys. Chem. A* **1999**, *103*, 1547−1552.
(28) Neubert, A.; Zmbov, K. F. *Trans. Faraday Soc.* **1974**, *70*, 2219.
(29) Piacente, V.; Gingerich, K. A. *High Temp. Sci.* **1977**, *9*, 189.
(30) Busse, B.; Weil, K. G. *Angew. Chem., Int. Ed. Engl.* **1979**, *18*, 629.
(31) Busse, B.; Weil, K. G. *Ber. Bunsen-Ges. Phys. Chem.* **1981**, *85*, 309.
(32) Scheuring, T.; Weil, K. G. *Int. J. Mass. Spectrom. Ion Phys.* **1983**, *47*, 227.
(33) Schwerdtfeger, P.; Dolg, M.; Schwarz, W. H. E. *J. Chem. Phys.* **1989**, *91*, 1762.
(34) Ziegler, T.; Snijders, J. G.; Baerends, E. J. *J. Chem. Phys.* **1981**, *74*, 1271.
(35) Gollisch, H. *J. Phys. B: At. Mol. Phys.* **1982**, *15*, 2569.
(36) de Jong, G. T.; Visscher, L. *Theor. Chem. Acc.* **2002**, *107*, 304.
(37) Saue, T.; Fægri, K.; Helgaker, T.; Gropen, O. *Mol. Phys.* **1997**, *91*, 937.
(38) Fossgaard, O.; Gropen, O.; Eliav, E.; Saue, T. *J. Chem. Phys.* **2003**, *119*, 9355.
(39) Tong, G. S.-M.; Cheung, A. S.-C. *J. Phys. Chem. A* **2002**, *106*, 11637.
(40) Belpassi, L.; Tarantelli, F.; Sgamellotti, A.; Quiney, H. M. *J. Chem. Phys.* **2005**, *122*, 184109.
(41) Belpassi, L.; Storchi, L.; Tarantelli, F.; Sgamellotti, A.; Quiney, H. M. *Future Gener. Comput. Syst.* **2004**, *20*, 739.
(42) Quiney, H. M.; Belanzoni, P. *J. Chem. Phys.* **2002**, *117*, 5550.
(43) Bader, R. F. W. *Atoms in Molecules. A Quantum Theory*; Cambridge University Press: Oxford, U.K., 1991.
(44) Grant, I. P.; Quiney, H. M. *Phys. Rev. A* **2000**, *62*, 022508.
(45) Quiney, H. M.; Skaane, H.; Grant, I. P. *Adv. Quantum Chem.* **1999**, *32*, 1.
(46) Grant, I. P.; Quiney, H. M. *Int. J. Quantum Chem.* **2000**, *80*, 283.
(47) McMurchie, L. E.; Davidson, E. R. *J. Comput. Phys.* **1978**, *26*, 218.
(48) Almlöf, J. *J. Chem. Phys.* **1996**, *104*, 4685. Ahmadi, G. R.; Almlöf, J. *Chem. Phys. Lett.* **1996**, *246*, 364.
(49) Quiney, H. M.; Belanzoni, P.; Sgamellotti, A *Theor. Chem. Acc.* **2002**, *108*, 113.
(50) Dunning, T. H., Jr. *J. Chem. Phys.* **1989**, *90*, 1007.
(51) Woon, D. E.; Dunning, T. H., Jr. To be published. The basis set is available at http://www.emsl.pnl.gov/forms/basisform.html.
(52) Blaudeau, J.-P.; McGrath, M. P.; Curtiss, L. A.; Radom, L. *J. Chem. Phys.* **1997**, *107*, 5016.
(53) Faegri, K. Department of Chemistry, University of Oslo; http://folk.uio.no/knutf/bases/four/TCA.2001.Rb-Xe.
(54) Fossgaard, O.; Gropen, O.; Corral Valero, M.; Saue, T. *J. Chem. Phys.* **2003**, *118*, 10418.
(55) Slater, J. C. *Phys. Rev.* **1951**, *81*, 385.
(56) Becke, A. D. *Phys. Rev. A* **1988**, *38*, 3098.
(57) Perdew, J. P. *Phys. Rev. B* **1986**, *33*, 8822.
(58) Hamprecht, F. A.; Cohen, A. J.; Tozer, D. J.; Handy, N. C. *J. Chem. Phys.* **1998**, *109*, 6264.
(59) Lee, C.; Yang, W.; Parr, R. G. *Phys. Rev. B* **1988**, *37*, 785.
(60) Functionals were obtained from the Density Functional Repository as developed and distributed by the Quantum Chemistry Group, CCLRC Daresbury Laboratory, Daresbury, Cheshire, WA4 4AD United Kingdom: http://www.cse.clrc.ac.uk/qcg/dft.
(61) Dunham, J. L. *Phys. Rev.* **1932**, *41*, 721.
(62) Moore, C. E. Ionization potentials and ionization limits derived from the analyses of optical spectra. *Natl. Stand. Ref. Data Ser. (U. S. Natl. Bur. Stand.)* **1970**, *34*, 1.
(63) Hotop, H.; Lineberger, W. C. *J. Phys. Chem. Ref. Data* **1985**, *14*, 731.
(64) Langhoff, S. R.; Bauschlicher, C. W., Jr.; Partridge, H. *J. Chem. Phys.* **1986**, *84*, 1687.
(65) Becke, A. D. *J. Chem. Phys.* **1988**, *88*, 2547.
(66) Mulliken, R. S. *J. Chem. Phys.* **1955**, *23*, 1833.
(67) Chirlian, L. E.; Francl, M. M. *J. Comput. Chem.* **1987**, *8*, 894−905.
(68) Belpassi, L.; Tarantelli, F.; Sgamellotti, A.; Quiney, H. M. To be published.
(69) Szefczyk, B.; Sokalski, W. A.; Leszczynski, J. *J. Chem. Phys.* **2002**, *117*, 6952.
(70) Wolfram, S. *The Mathematica Book*, 4th ed.; Wolfram Media; Cambridge University Press: New York, 1999.
(71) Parr, R. G.; Yang, W. *Density-functional Theory of Atoms and Molecules*; Oxford University Press: Oxford, 1989.
(72) Sinnokrot, M. O.; Sherrill, C. D. *J. Chem. Phys.* **2001**, *115*, 2439.
(73) Neugebauer, J.; Hess, B. A. *J. Chem. Phys.* **2003**, *118*, 7215.
(74) Schneider, W.; Thiel, W. *Chem. Phys. Lett.* **1989**, *157*, 367.
(75) Miani, A.; Cané, E.; Palmieri, P.; Trombetti, A. *J. Chem. Phys.* **2000**, *112*, 248.
(76) Johnson, B. G.; Gill, P. M. W.; Pople, J. A. *J. Chem. Phys.* **1993**, *98*, 5612.
(77) Schwerdtfeger, P.; Pernpointner, M.; Laerdahl, J. K. *J. Chem. Phys.* **1999**, *111*, 3357.
(78) Bader, R. F. W. *Chem. Rev.* **1991**, *91*, 893−928.
(79) Gervasio, G.; Bianchi, R.; Marabello, D. *Chem. Phys. Lett.* **2004**, *387*, 481−484.
(80) Bader, R. F. W.; Matta, C. F. *Inorg. Chem.* **2001**, *40*, 5603.
(81) Llusar, R.; Beltrán, A.; Andrés, J.; Fuster, F.; Silvi, B. *J. Phys. Chem. A* **2001**, *105*, 9460.
(82) Pilme, J.; Silvi, B.; Alikhani, M. E. *J. Phys. Chem. A* **2003**, *107*, 4506.
(83) Groen, C. P.; Oskam, A. *Inorg. Chem.* **2000**, *39*, 6001.
(84) Jansen, G.; Schubart, M.; Findeis, B.; Gade, L. H.; Scowen, I. J.; McPartlin, M. *J. Am. Chem. Soc.* **1998**, *120*, 7239.
(85) Frenking, G.; Fröhlich, N. *Chem. Rev.* **2000**, *100*, 717.
(86) Müller-Rösing, M.-C.; Schulz, A.; Hargittai, M. *J. Am. Chem. Soc.* **2005**, *127*, 8133.
(87) Berski, S.; Latajka, Z.; Andrés, J. *Chem. Phys. Lett.* **2002**, *356*, 483.
(88) Fortunelli, A.; Germano, G. *J. Phys. Chem. A* **2000**, *104*, 10834.
(89) Aray, Y.; Rodriguez, J.; Vega, D. *J. Phys. Chem. B* **2000**, *104*, 4608.
(90) Macchi, P.; Proserpio, D. M.; Sironi, A. *J. Am. Chem. Soc.* **1998**, *120*, 13429.
(91) Macchi, P.; Sironi, A. *Coord. Chem. Rev.* **2003**, *238−239*, 383.
(92) Bader, R. F. W.; Gillespie, R. J.; Martin, F. *Chem. Phys. Lett.* **1998**, *290*, 488.
(93) Vyboishchikov, S. F.; Sierraalta, A.; Frenking, G. *J. Comput. Chem.* **1996**, *18*, 416.
(94) Kohout, M.; Savin, A.; Preuss, H. *J. Chem. Phys.* **1991**, *95*, 1928.
(95) Sagar, R. P.; Ku, A. C. T.; Smith, V. H.; Simas, A. M. *J. Chem. Phys.* **1988**, *88*, 4367.

(96) Bader, R. F.; Heard, G. L. *J. Chem. Phys.* **1999**, *111*, 8789 (and references therein).
(97) Shi, Z.; Boyd, R. J. *J. Chem. Phys.* **1988**, *88*, 4375.
(98) Cortés-Guzmán, F.; Bader, R. F. W. *Coord. Chem. Rev.* **2005**, *249*, 633−662. Silvi, B.; Gatti, C. *J. Phys. Chem. A* **2000**, *104*, 947.
(99) Cremer, D.; Kraka, E. *Angew. Chem., Int. Ed. Engl.* **1984**, *23*, 67.
(100) Cooke, S. A.; Gerry, M. *J. Am. Chem. Soc.* **2004**, *126*, 17000.
(101) Bader, R. F. W. *J. Phys. Chem. A* **1998**, *102*, 7314.
(102) Abramov, Y. A. *Acta Crystallogr., Sect. A* **1997**, *53*, 264.
(103) Macchi, P.; Garlaschelli, L.; Sironi, A. *J. Am. Chem. Soc.* **2002**, *124*, 14173.
(104) McLean, A. D.; Chandler, G. S. *J. Chem. Phys.* **1980**, *72*, 5639.
(105) Glukhovstev, M. N.; Pross, A.; McGrath, M. P.; Radom, L. *J. Chem. Phys.* **1995**, *103*, 1878.
(106) Huber, K. P.; Herzberg, G. *Molecular Spectra and Molecular Structure IV. Constants of Diatomic Molecules*; Van Nostrand Reinhold: New York, 1979.